

Article

# Synthesis and Characterisation of Metal Oxide Nanostructures Using Choline/Linear Alkyl Carboxylate Deep Eutectic Solvents

Omar Gómez Rojas and Tadachika Nakayama \*

Extreme Energy-Density Research Institute, Nagaoka University of Technology, 1603-1 Kamitomiokamachi, Nagaoka, Niigata Prefecture 940-2188, Japan; omargr@vos.nagaokaut.ac.jp

\* Correspondence: nky15@vos.nagaokaut.ac.jp

Received: 12 November 2020; Accepted: 6 December 2020; Published: 8 December 2020



**Abstract:** The synthesis of  $\text{YBa}_2\text{Cu}_3\text{O}_{7-x}$  (YBCO or 123) was carried out via the use of a variety of deep eutectic solvents (DESs), all formed by the interaction of choline hydroxide (as the cation source) and alkyl carboxylic acids with  $C_n\text{H}_{2n+1}$  ranging from  $n = 2$  to  $n = 10$ , namely acetic acid, propionic acid, butyric acid, pentanoic acid, nonanoic acid, and decanoic acid, as providers of the anion, all prepared in equimolar solutions. The behaviour of the synthetic media and the resulting morphology displayed by the crystallite product, using different molar ratios of DESs ( $X$ ):1  $\text{YBaCu}$  metal nitrates mixes, with  $x$  values of  $20 \leq x \leq 60$ , is also reported. Synthetic performance results show a tendency to generate higher total phase percentage of the desired crystal with the increase of the alkyl chain length of the carboxylic acid up to butyric acid (92% belonging to the metal oxide), after which no enhancement was observed. Furthermore, the synthetic performance of the remaining, i.e., DES formed with pentanoic acid to decanoic acid, displayed a constant decay in total desired phase percentage belonging to the metal oxide. Morphological results were also analysed for all DESs ( $X$ ):1  $\text{YBaCu}$  metal nitrates mixes, with  $x$  values of  $20 \leq x \leq 60$ . Well defined plate-like particles were generally observed however, in some cases fused plate-like particles of significantly bigger size were observed.

**Keywords:** deep eutectic mixtures; metal oxide; self-assemble; crystal morphology; carboxylic acids

## 1. Introduction

Metal oxides are a type of material that has plethora of applications, consequently, scientist world-wide have generated numerous synthetic routes of producing them [1]. Among them, developments such as the discovery of high-temperature superconductors has drawn wide attention into multicomponent compounds with more complicated assemblies [2]. Perhaps the most relevant superconductor to date is  $\text{YBa}_2\text{Cu}_3\text{O}_{7-x}$  (YBCO or 123), owing to it be the first superconductor with a superconductive transitioning critical temperature above that from liquid nitrogen ( $B_p = 77$  K), specifically for  $\text{YBa}_2\text{Cu}_3\text{O}_{7-\delta}$  when  $0 < \delta < 0.2$  the critical temperature is slightly above 90 K [3]. However, more recently, emphasis on the synthesis of not only novel functional materials, but also on creating more complex and intricate superstructures, has been given, owing to how intrinsically interconnected are properties exhibited by the material and the resulting morphology of the product [4]. An example of this is presented by the generation of ultra-thin surfaces and interface layers of metallic films, cuprates and metallic interfaces, which relevance relies on the capability to in-depth study the superconductor-insulator transition [5]. To produce materials with specific size, shape, and functionality, there are two different approaches. The first, top-down, functional materials are produced from bulk as a starter, and by techniques such as lithographic techniques [6], ball milling [7], etching [8], sputtering [9], etc. It will be transformed and

constrained to the micro–nano scale. The second, bottom-up, starter materials belong to chemical reactants or molecules, and by allowing and controlling their interactions, self-assembled, via techniques such as sol-gel processes [10], hydrothermal [11], spray pyrolysis [12], etc., engender growth up to the desired point.

Within bottom-up synthetic approaches for the synthesis of metal oxides with specific size, shape and functionality, wet chemistry synthetic routes have flourished, due to their chemical flexibility, with a plethora of precursors and surfactants to be chosen, and the possibility to vary reaction times and temperatures at which the synthesis is being carried out [13,14].

A synthetic method that has been used ever more often, is the synthesis of metal oxides via the use of ionic liquid (IL)/deep eutectic solvents (DESs) [15–17]. This methodology can be dissected in two different segments. The first belongs to the early stages of the synthetic procedure, defined by the formation of metal nanoparticles by being chelated by the capping agent, provided by the IL or DES. The most standard procedure of this process to be found in literature is as follows: commonly metal nitrates, previously dissolved in water, will be added to the IL/DES in question. Then the solution, IL with metal nitrates, will be dehydrated to replace bonded molecules of water for the capping agent. Finally, after normally 2 h of dehydration at 80 °C, the second step of the reaction occurs, namely calcination [18]. Despite the fact that the IL/DES can provide chemical flexibility, with the IL/DES being produced by diverse chemical reactants [19,20], the capability to chelate and upkeep in solution metal cations [21], and their thermal stability [22], no study, to the extent of our knowledge, has been done to explore the synthesis of metal oxides while generating variations in the resulting morphology of the crystal, by varying sizes of the anion employed to form the IL/DES, and dehydrating the initial solution, composed of the IL/DES and dissolved metal nitrates, at different temperatures, hence generating dissimilarities into the self-assembled structure being produced between the IL/DES and the metal nanoparticle, which upon calcination could deliver significant differences of the crystallite obtained.

Therefore, this work focuses on the synthesis of a metal oxide via several DES mixes, all containing choline hydroxide as the source of a cation, and acetic acid, propionic acid, butyric acid, pentanoic acid, nonanoic acid, and decanoic acid as the sources of anions. Also, initial conditions, specifically the dehydration process, was carried out at different temperatures, viz. 80, 150, 180, 250, and 300 °C, and held for 6 h before calcining. After calcination and collection of the sample, the product was characterised via powder X-ray diffraction patterns, and scanning electron microscopy images.

## 2. Results

### 2.1. Synthetic Performance of DES (X):1 YBaCu Metal Nitrates Mixes, through Variation of the Carboxylic Acid Alkyl Chain Lengths

Several DES were synthesised with the purpose of analysing their synthetic performance of the synthesis of a metal oxide, with emphasis on the effect of the size of the anion composing the DES, and the total phase percentage obtained of the desired functional material. Choline derived compounds have already proved proficiency in the synthesis of metal oxides [17], consequently choline hydroxide was chosen as the source of a cation and stabilizer. In order to vary the alkyl chain length, therefore, the size of the molecule containing the anion employed in the reaction, acetic acid ( $\text{CH}_3\text{COOH}$ ), propionic acid ( $\text{CH}_3\text{CH}_2\text{COOH}$ ), butyric acid ( $\text{CH}_3(\text{CH}_2)_2\text{COOH}$ ), pentanoic acid ( $\text{CH}_3(\text{CH}_2)_3\text{COOH}$ ), nonanoic acid ( $\text{CH}_3(\text{CH}_2)_7\text{COOH}$ ), and decanoic acid ( $\text{CH}_3(\text{CH}_2)_8\text{COOH}$ ) were chosen.

Their synthetic performance was evaluated using powder diffraction patterns and Rietveld refinement, to establish the total phase percentage obtained of the desired crystal, namely YBCO (123). Initially, reactions using DES 1:1 YBaCu metal nitrates mixes were carried out, however, the volume of the DES was not enough to provide a suitable environment for the synthesis of the metal oxide. Consequently, molar ratios of the DESs vs. metal nitrates were increased, from 10:1 to 80:1, and their synthetic performance analysed. The results can be seen in Figure 1.

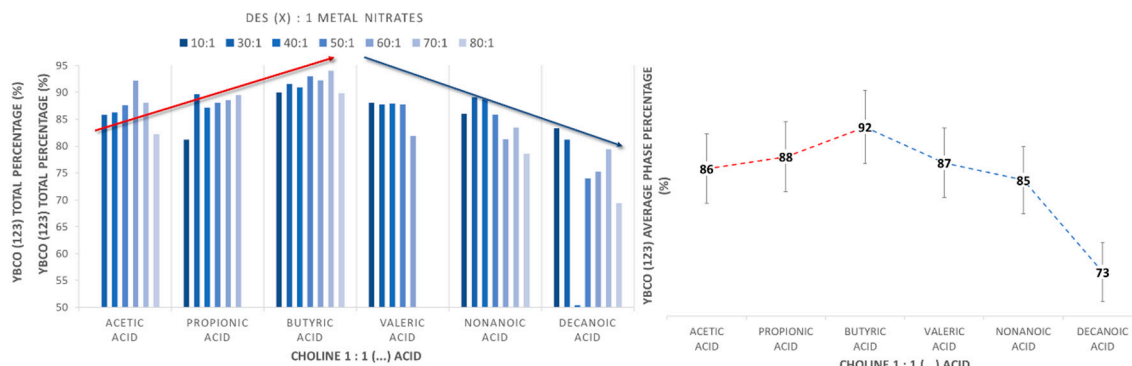


**Figure 1.** (Left) Summary of the maximum percentage of the metal oxide  $\text{YBa}_2\text{Cu}_3\text{O}_{7-x}$  (YBCO or 123) obtained, via different deep eutectic solvents (DESs) formed by choline hydroxide and acetic/propionic/butyric/pentanoic/nonanoic/decanoic acid. The red arrow indicates a positive trend towards higher total phase percentage obtained, whereas the blue arrow indicates an opposite trend. (Right) Graphic indicating the average total phase percentage obtained per segment of DES.

Individually, the performance of each of the DES ( $X$ ):1 YBaCu metal nitrates mixes, with  $x$  values from  $10 \leq x \leq 80$ , does not exhibit any linear trend that can be easily described towards higher or lower total phase percentages of YBCO (123), with regards of using lower or greater molar ratio discrepancies between the DESs and YBaCu metal nitrates. Nonetheless such results will be discussed in detail further on. However, when the data is analysed by blocks rather than the individual performance of each mix, taking into account the average total phase percentage obtained by a single DES in the whole series of reactions (Figure 1 right), it is clear that, the average total phase percentage increases with the increase of the alkyl chain of the carboxylic acid employed, but only up to the point of  $C_n\text{H}_{2n+1} n = 4$  (Figure 1 red arrow), with values resulting in 86.4% for the DES formed with acetic acid, 87.9% for that DES with propionic acid, and 91.6% using butyric acid as the source of anion. From that point onwards,  $C_n\text{H}_{2n+1}$  ranging from  $n = 5$  to  $n = 10$  (Figure 1 blue arrow), the average total phase percentage continuously decreases, with the corresponding values being 87.1% for the DES with pentanoic acid, 85.0% for that DES with nonanoic acid, and 73.5% when decanoic acid is used (Figure 1).

In order to perform a far more detailed analysis of the synthetic performance displayed by the DES employed for the synthesis of the metal oxide, each series of reactions carried out with every DES will be described individually. Additionally, to establish the effect of using anion sources with variation of alkyl chain lengths, and how differences in the initial interaction between the metal cation and the DES, generated by the variance of the anion source, affect the resultant morphology shown by the crystallites that were synthesised, an SEM analysis was performed. For this purpose, samples in the form of fine powder were placed on the top of a sticky conductive carbon tab attached to the top of an aluminium sample stub. To analyse the morphology, samples were deposited very carefully on top of the carbon sticky layer and introduced to the cavity of the SEM, where SEM micrographs were taken. Also, for comparison and a better description of size distribution of the sample, hundred particles were measured per SEM micrograph taken. Using this data, histograms were produced and can be found in Figures S1–S9, as well as maximum and minimum crystallite sizes measured also being reported and will be discussed along the text. Finally, due to the length of work here presented, and being the focus of this work the report of changes in the resultant crystal morphology, added to the synthetic efficiency of the DES to produce the desired crystal composition (YBCO (123)), an in-depth analysis of other crystal compositions found during Rietveld analysis, performed on the powder diffraction patterns, is not discussed in the main text. However, total phase percentages, obtained via Rietveld refinement, belonging to YBCO (123) and other crystal compositions uncovered in the powder diffraction patterns, mainly  $\text{CuO}$ ,  $\text{Y}_2\text{BaCuO}_5$ ,  $\text{Y}_{0.5}\text{Ba}_3\text{Cu}_{1.5}\text{O}_{5.5}$ , and  $\text{Ba}_{0.98}\text{CuO}_{2.07}$ , can be found in Tables S2–S7.

## 2.2. Synthetic Performance of Choline Hydroxide 1:1 Acetic Acid, DES (X):1 YBaCu Metal Nitrates Mixes, with $x$ Values of $20 \leq x \leq 60$

Due to the vast amount of information collected, it was decided that each individual analysis was going to be done in the range of  $x$  values from 20 to 60. The synthetic performance displayed by the DES composed of choline hydroxide 1:1 acetic acid, linearly improves as larger molar ratio of de DES vs. YBaCu metal nitrates are used in the reaction, providing a total phase percentage of YBCO (123) of 82% for  $x = 10$ , 86% for  $x = 20$ , 86% for  $x = 30$ , 88% for  $x = 40$ , 88% for  $x = 50$ , and 92% for  $x = 60$  (Figure 2d). On the other hand, crystallite sizes also shown some differences, displaying smaller and a more uniform size distribution of crystallites with  $x$  values of 20 and 30 (Figure 2c), with no particular shape (Figure 2a,b), and with an average crystallite size of 553 and 507 nm for  $x = 20$  and 30, respectively (Figure 2c). However, crystallite sizes tend to increase with the increase of  $x$  values, viz.  $x = 40$  to 60, as well as size distribution being broader than that exhibited by lower  $x$  values, namely  $x = 20$  and 30, having an average size of the crystallites of 640, 758, and 1454 nm for  $x = 40$ , 50, and 60, respectively (Figure 2c).

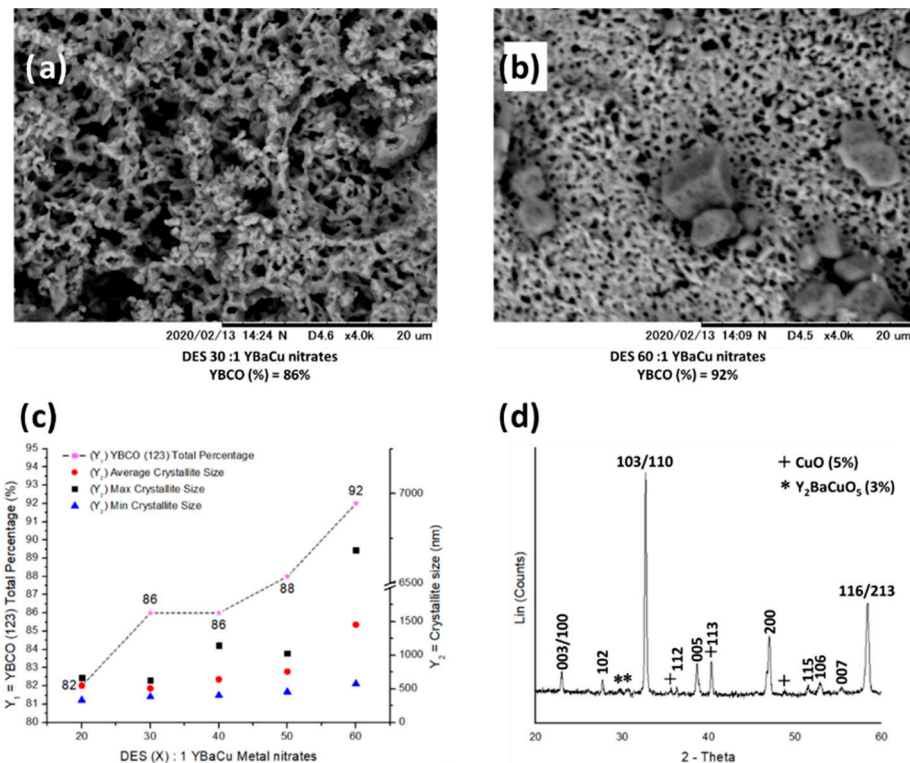


**Figure 2.** (a,b) Scanning Electron Microscopy (SEM) micrographs showing the morphology exhibited by the crystallites, synthesised using choline hydroxide 1:1 acetic acid and molar ratios of (a) DES 30:1 YBaCu metal nitrates, and (b) DES 60:1 YBaCu metal nitrates. (c) graphical representation of the total phase percentage of YBCO (123), and crystallite sizes per DES (X):1 YBaCu metal nitrates molar ratios use in the reaction, with  $x$  values of  $20 \leq x \leq 60$ . (d) indexed power diffraction pattern of the synthesis of YBCO (123) via DES 60:1 YBaCu metal nitrates.

## 2.3. Synthetic Performance of Choline Hydroxide 1:1 Propionic Acid, DES (X):1 YBaCu Metal Nitrates Mixes, with $x$ Values of $20 \leq x \leq 60$

There is a stark contrast between the synthetic performance, and morphology exhibited by the crystallites obtained using DES composed of choline hydroxide 1:1 propionic acid, compared to those results obtained by the DES using acetic acid as the source of the anion. Firstly, the synthetic performance is better at lower  $x$  values, e.g.,  $x = 10 > 20 > 30$ , with YBCO (123) total phase percentage values of 91%, 90%, and 87% correspondingly, compared to 82% and 86% obtained by the DES with

acetic acid at  $x = 10$ , and 20–30, respectively (Figure 3d). From that point onwards YBCO (123) total phase percentage values increased up to 88% for  $x = 50$ , and 89% for  $x = 60$  (Figure 3d). Secondly, opposed to results seen by the DES composed by acetic acid, with crystallites increasing in size with  $x$  values also increasing, with propionic acid employed as the source of the anion, crystallite sizes are significantly bigger at lower  $x$  values, with average crystallite sizes of 650 nm for  $x = 20$  and 1151 nm for  $x = 30$  and 1009 nm for  $x = 40$ , and will gradually decrease in size with  $x$  values increasing, with their respective average crystallite sizes being 623 nm and 465 nm for  $x = 50$  and  $x = 60$  correspondingly (Figure 3c). Additionally, morphology exhibited by the crystallites resemble a plate-like morphology, especially at lower  $x$  values, viz.  $x = 20$ –30, and changes towards a mix of plate-like particles added to amorphous units at higher  $x$  values, namely  $x = 40$ –60. (Figure 3a,b).

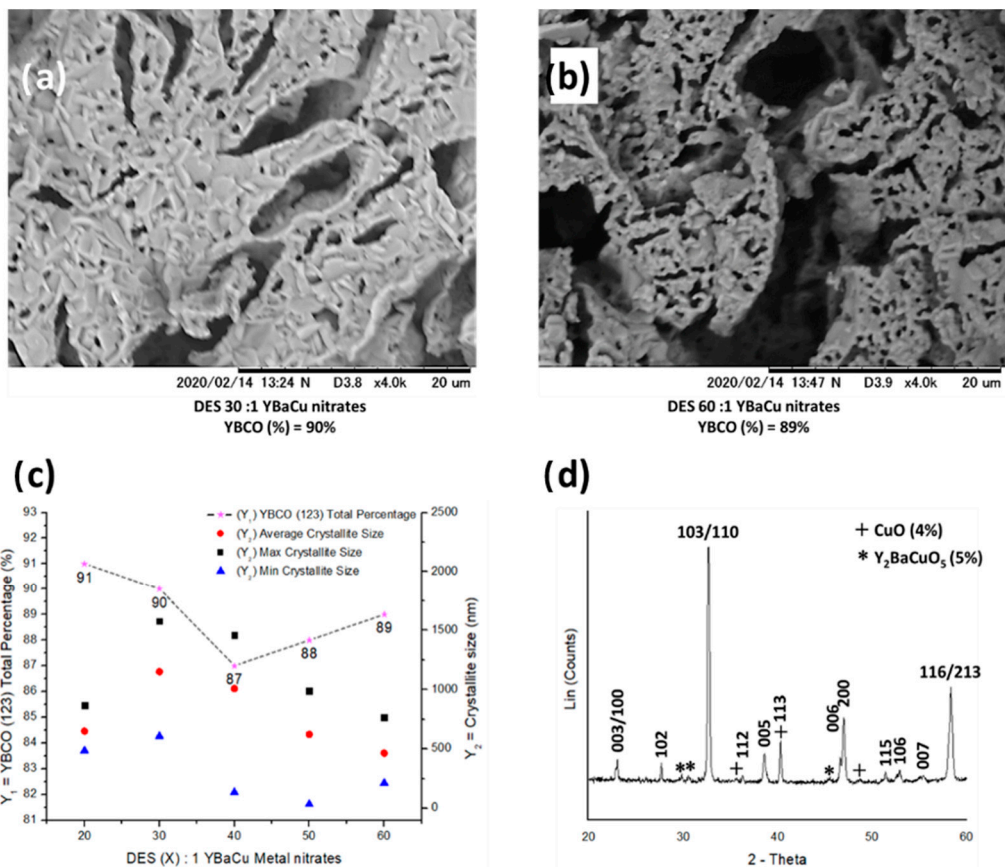


**Figure 3.** (a,b) SEM micrographs showing the morphology exhibited by the crystallites, synthesised using choline hydroxide 1:1 propionic acid and molar ratios of (a) DES 30:1 YBaCu metal nitrates, and (b) DES 60:1 YBaCu metal nitrates. (c) graphical representation of the total phase percentage of YBCO (123), and crystallite sizes per DES (X):1 YBaCu metal nitrates molar ratios use in the reaction, with  $x$  values of  $20 \leq x \leq 60$ . (d) indexed power diffraction pattern of the synthesis of YBCO (123) via DES 20:1 YBaCu metal nitrates.

#### 2.4. Synthetic Performance of Choline Hydroxide 1:1 Butyric Acid, DES (X):1 YBaCu Metal Nitrates Mixes, with $x$ Values of $20 \leq x \leq 60$

The synthetic performance displayed by the mix of choline hydroxide 1:1 butyric acid was the best obtained among all the other combinations, with every DES (X):1 YBaCu metal nitrates mixes, with  $x$  values of  $20 \leq x \leq 60$ , with all above 90% of the total phase percentage belonging to the metal oxide, specifically 91%, 92%, 91%, 93%, and 92% for  $x$  values ranging from 20 to 60 (Figure 4d). Morphological results are similar to those seen by the DES made with propionic acid, with crystallite sizes being bigger at lower  $x$  values, and decreasing in size while  $x$  values get higher. However, in this

particular case the average crystallite size remains rather stable, with variation of  $\pm 300$  nm, with values being 1173, 1077, 837, 985, and 995 nm for  $x = 20$  to 60, respectively. In spite of that, crystallite size changes are evidently seen by the maximum crystallite size measured, being 2650, 1889, 1345, 1587, and 1888 nm for  $x = 20$  to 60, correspondingly. (Figure 4c) Also, the morphology exhibited along the whole series of reactions resemble plate-like particles with road-like particles, in contrast to results seen by the DES formed with propionic acid, where the plate-like crystal morphology seems to be disrupted at higher  $x$  values, producing shapeless particles (Figure 4a,b).

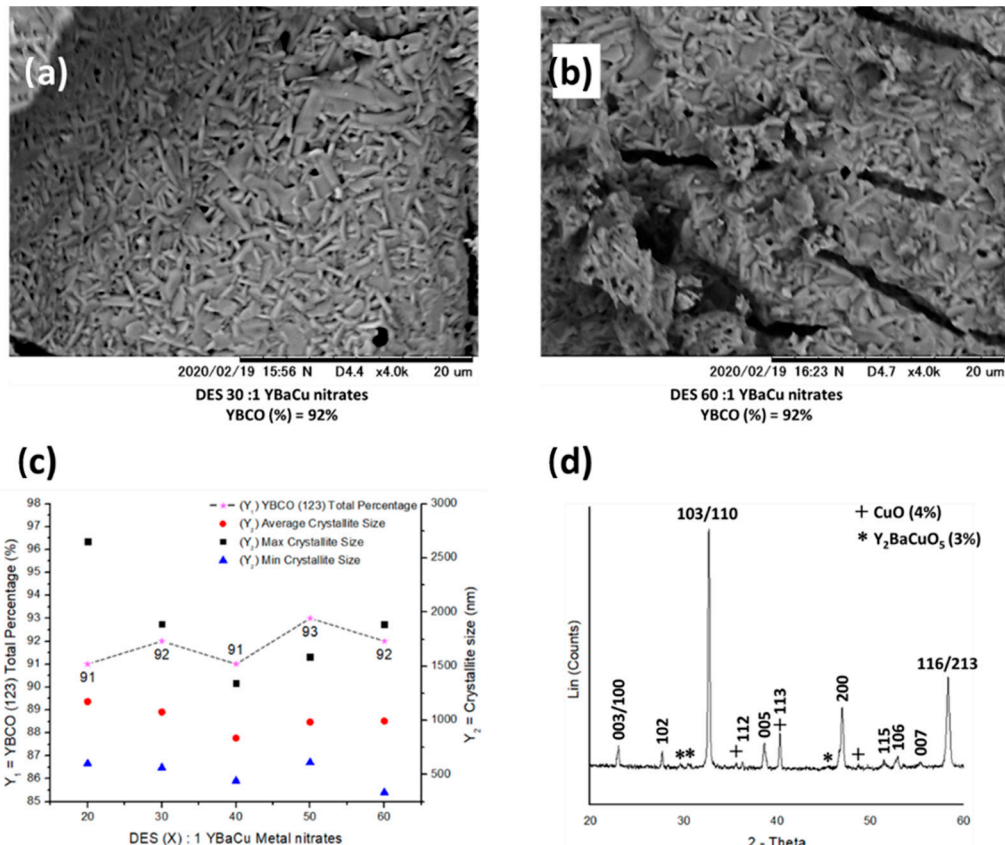


**Figure 4.** (a,b) SEM micrographs showing the morphology exhibited by the crystallites, synthesised using choline hydroxide 1:1 butyric acid and molar ratios of (a) DES 30:1 YBaCu metal nitrates, and (b) DES 60:1 YBaCu metal nitrates. (c) graphical representation of the total phase percentage of YBCO (123), and crystallite sizes per DES (X):1 YBaCu metal nitrates molar ratios use in the reaction, with  $x$  values of  $20 \leq x \leq 60$ . (d) indexed power diffraction pattern of the synthesis of YBCO (123) via DES 50:1 YBaCu metal nitrates.

## 2.5. Synthetic Performance of Choline Hydroxide 1:1 Pentanoic Acid, DES (X):1 YBaCu Metal Nitrates Mixes, with $x$ Values of $20 \leq x \leq 60$

As described above, the synthetic performance of the reactions from this point onwards lessens, in terms of total phase percentage of the desired metal oxide being obtained. Besides, with the mix of choline hydroxide 1:1 pentanoic acid, the total phase percentage obtained leans towards lower values with  $x$  values increasing in DES (X):1 YBaCu metal nitrates mixes, with  $x$  values of  $20 \leq x \leq 60$ , providing the corresponding values of 89% for  $x = 20$ , 88% for  $x = 30\text{--}50\%$ , and 82% for  $x = 60\%$  (Figure 5d). Another feature observed is the size of the crystallite obtained, with a constant decrease in the average crystallite size with  $x$  values also being increased, having average crystallite size values of 1380 nm for  $x = 20$ , 933 nm for  $x = 30$ , 572 nm for  $x = 40$ , 783 nm for  $x = 50$ , and 523 nm for  $x = 60$  (Figure 5c). While the morphology of the crystallites in question resemble plate-like particles (Figure 5a,b), uniformity of the crystallite size is gained with  $x$  values being increased. This is notorious

in Figure 5c, having maximum crystallite size, average crystallite size, and minimum crystallite size measured standing all close to each other.

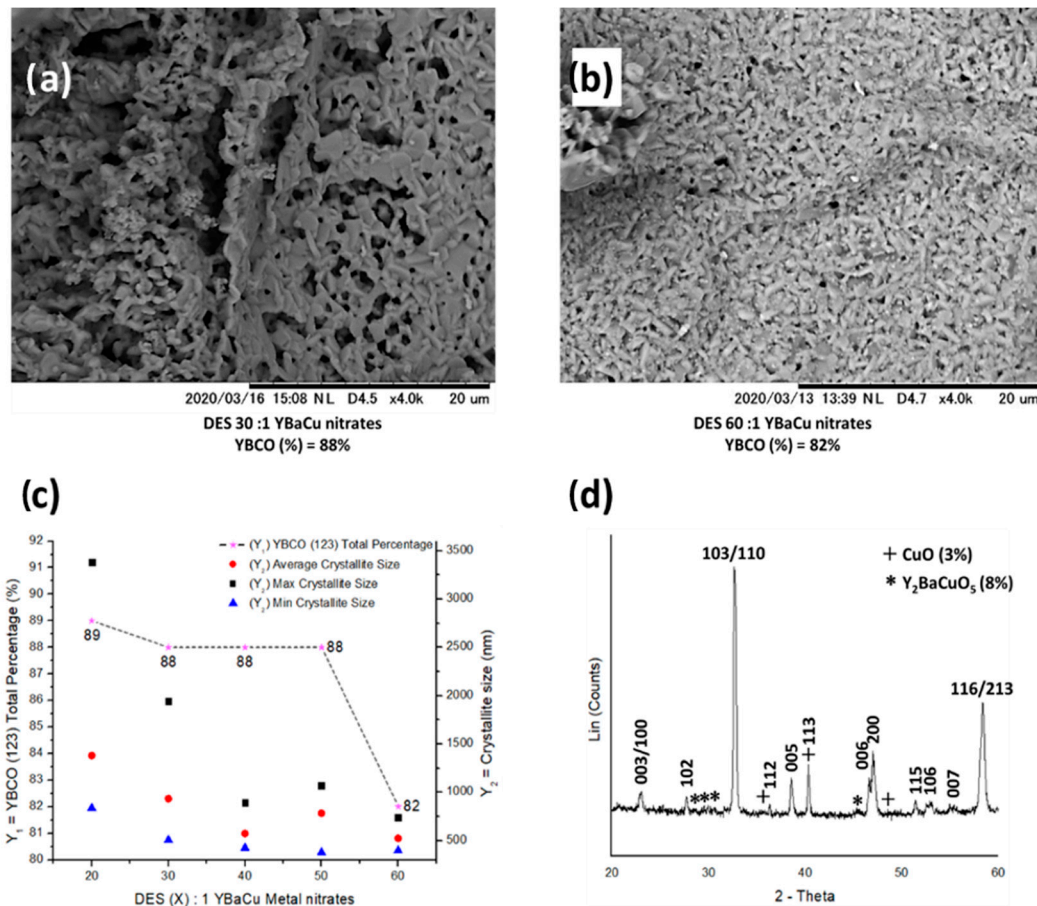


**Figure 5.** (a,b) SEM micrographs showing the morphology exhibited by the crystallites, synthesised using choline hydroxide 1:1 pentanoic acid and molar ratios of (a) DES 30:1 YBaCu metal nitrates, and (b) DES 60:1 YBaCu metal nitrates. (c) graphical representation of the total phase percentage of YBCO (123), and crystallite sizes per DES ( $X$ ):1 YBaCu metal nitrates molar ratios use in the reaction, with  $x$  values of  $20 \leq x \leq 60$ . (d) indexed power diffraction pattern of the synthesis of YBCO (123) via DES 20:1 YBaCu metal nitrates.

#### 2.6. Synthetic Performance of Choline Hydroxide 1:1 Nonanoic Acid, DES ( $X$ ):1 YBaCu Metal Nitrates Mixes, with $x$ Values of $20 \leq x \leq 60$ , and Choline Hydroxide 1:1 Decanoic Acid, DES ( $X$ ):1 YBaCu Metal Nitrates Mixes, with $x$ Values of $20 \leq x \leq 60$ .

For the sake of simplicity and due to the similarity in results obtained by these two DESs, it was decided to describe them together (Figure 6 and Figure S10). In terms of synthetic performance, nonanoic acid still exhibited a somewhat good performance with values being 87%, 89%, 86% and 81%, corresponding to  $x = 20$ ,  $x = 30\text{--}40$ ,  $x = 50$ , and  $x = 60$ , respectively (Figure 6d), whereas, the synthetic performance of the DES formed with decanoic acid can be described as poorly, barely obtaining 81% at its best, namely  $x = 30$  (Figure S10d). However, morphological results are both fairly similar (Figure 6 and Figure S10a,b), having shown bigger crystallites with lower  $x$  values, and a clear tendency towards smaller crystallites with the increase of  $x$  values. In both cases, the shape of the crystallites is clearly plate-like at  $x = 20$ , although with a predisposition of building more like a net of crystallites of lower dimension with  $X$  values increasing. In terms of average sizes values are 1059, 1220, 1310, 754, and 600 nm when the DES is formed with nonanoic acid and for  $x$  values ranging from 20 to 60,

correspondingly, and 1059, 1218, 1310, 493, and 600 nm while using the DES containing decanoic acid and for  $x$  values ranging from 20 to 60, respectively.

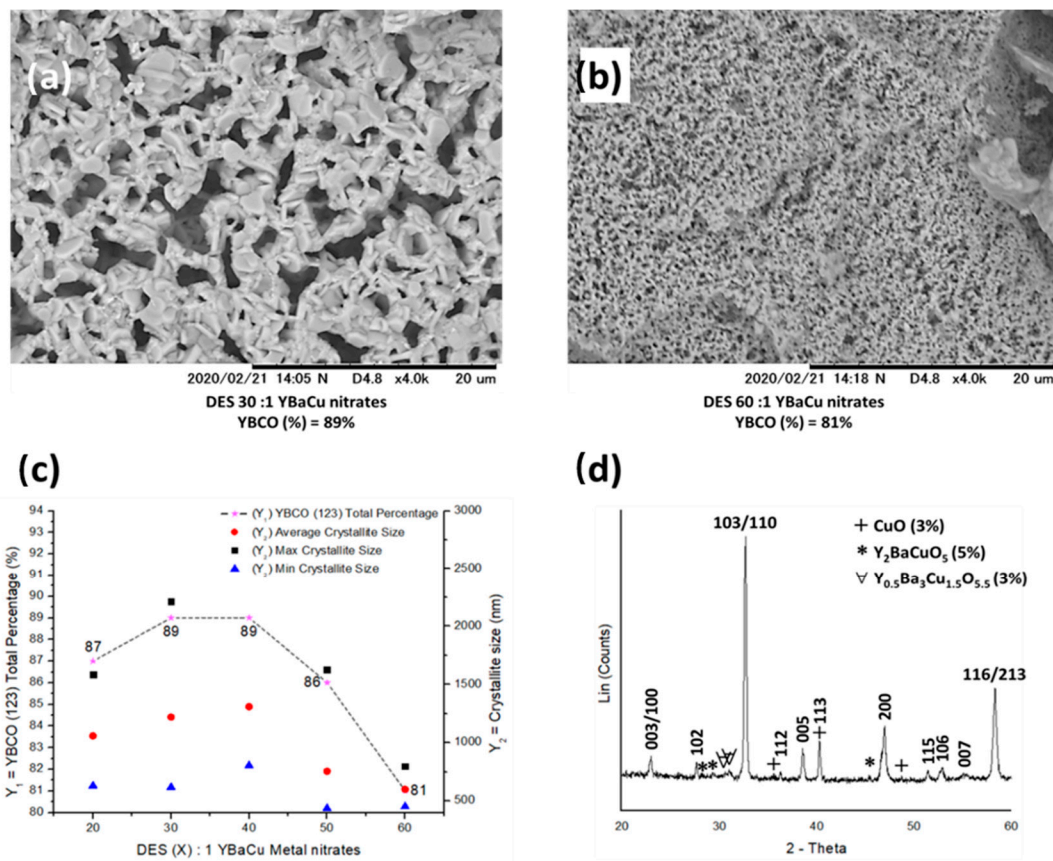


**Figure 6.** (a,b) SEM micrographs showing the morphology exhibited by the crystallites, synthesised using choline hydroxide 1:1 nonanoic acid and molar ratios of (a) DES 30:1 YBaCu metal nitrates, and (b) DES 60:1 YBaCu metal nitrates. (c) graphical representation of the total phase percentage of YBCO (123), and crystallite sizes per DES ( $X$ ):1 YBaCu metal nitrates molar ratios use in the reaction, with  $x$  values of  $20 \leq x \leq 60$ . (d) indexed power diffraction pattern of the synthesis of YBCO (123) via DES 30:1 YBaCu metal nitrates.

(Figure 6 and Figure S10c) It is also noteworthy to highlight the size uniformity obtained at higher  $x$  values however, it does come with a decrease in synthetic performance.

A summary of average crystallite sizes can be found in Table 1.

**Table 1.** Summary of crystallite sizes obtained by every DES and with different DES ( $X$ ):1 YBaCu metal nitrates molar ratios.

DES ( $X$ ):1 YBaCu Metal Nitrates	Average Crystallite Size (nm)						
	Choline Hydroxide 1:1 Acetic Acid	Choline Hydroxide 1:1 Propionic Acid	Choline Hydroxide 1:1 Butyric Acid	Choline Hydroxide 1:1 Pentanoic Acid	Choline Hydroxide 1:1 Nonanoic Acid	Choline Hydroxide 1:1 Decanoic Acid	
20	553	650	1173	1380	1059	1059	
30	507	1151	1077	933	1220	1218	
40	640	1009	837	572	1310	1310	
50	758	623	985	783	754	493	
60	1454	465	995	523	600	600	

## 2.7. Synthetic Performance of Choline Hydroxide 1:1 Acetic Acid, DES 60:1 YBaCu Metal Nitrates, Choline Hydroxide 1:1 Pentanoic Acid, DES 30:1 YBaCu Metal Nitrates, and Choline Hydroxide 1:1 Nonanoic Acid, DES 20:1 YBaCu Metal Nitrates Mixes, in Extraordinary Initial Conditions

The first thing that needs to be stated is what is considered extraordinary. To this day, the synthesis of metal oxides via ionic liquid/deep eutectic solvents has been performed with an initial dehydration process being carried out at 80 °C. However, no study, to the extent of our knowledge, has analysed the effect of the dehydration process being done and held at different temperatures, namely 150, 180, 250, and 300 °C. The reason behind choosing 150 °C is due to the fact that it is widely used in literature regarding crystal growth of metal nanoparticles [14], and is a temperature above acetic acid's boiling point of 117.9 °C [23], whereas 150, 250, and 300 °C were chosen owing to their proximity to the boiling points of pentanoic acid (186 °C), nonanoic acid (254 °C), and choline hydroxide (305 °C) [23]. It is known that, ionic liquids and deep eutectic solvents can form metal-chelated nanoparticles [21], and studies on the crystal formation of metal nanoparticles have highlighted that, initial conditions such as temperature, time at which the solution is being held, and the capping agent have influence on the size and shape of the metal nanoparticle being produced [14]. Here, we compare results in terms of micromorphology obtained in different initial conditions, viz. different temperatures (150, 180, 250, and 300 °C), and held in a hot plate for 6 h before calcination. After the given time was completed, the calcination process was carried out immediately.

### 2.7.1. Synthetic Performance of Choline Hydroxide 1:1 Acetic Acid, DES 60:1 YBaCu Metal Nitrates

The synthesis carried out using acetic acid as the source of the anion and chelating agent provides similar results, in terms of crystallite size, compared to those seen when the initial solution is dehydrated at 80 °C, with values of 1454 nm for 80 °C, 1189 nm for 150 °C, 1532 nm for 180 °C, and 2300 nm for 300 °C (Figure 7e). An exception is seen at 250 °C with an average crystallite size of 620 nm. However, in terms of micromorphology and synthetic performance, results do exhibit differences. When the initial solution is dehydrated at 80 °C, the micromorphology is composed mainly by crystallites with no specific shape, whereas results obtained at 150, 180, and 300 °C clearly displayed flat plate-like particles (Figure 7a–d). Furthermore, the sizes of those microparticles increased with the rise of dehydration temperature, providing average crystallite size values of 1189 nm at 150 °C, 1532 nm at 180 °C, and 2300 nm at 300 °C. These results did come at the expenses of the synthetic performance, with a YBCO (123) total phase percentage obtained of 92% at 80 °C, 75% at 150 °C, 76% at 180 °C, and 73% at 300 °C (Figure 7e). The reaction with dehydration process carried out at 250 °C, exhibited a mix between large sheets and small sphere-like nanoparticles, with a synthetic performance of 70% belonging to the desired metal oxide (Figure 7e).

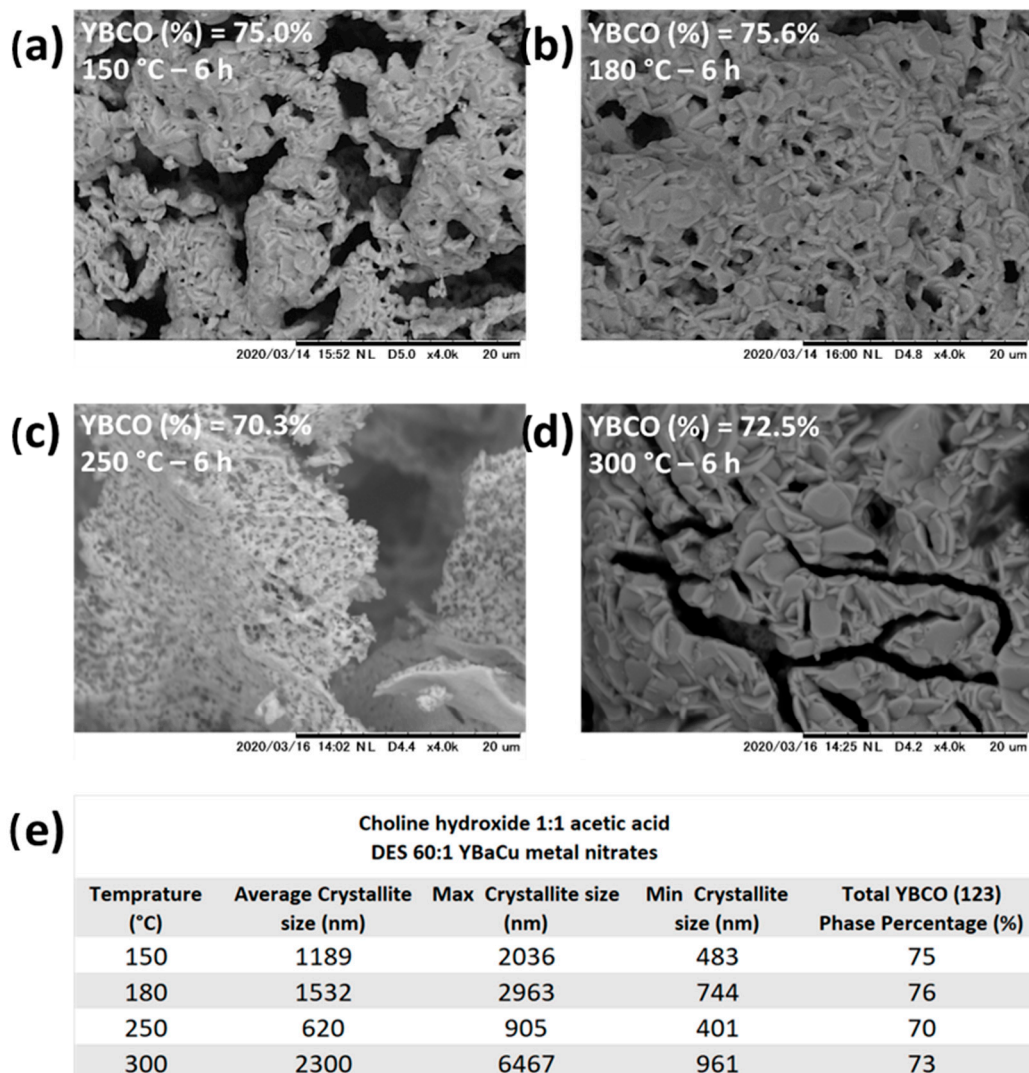


**Figure 7.** (a–d) SEM micrographs showing the morphology exhibited by the crystallites, synthesised using choline hydroxide 1:1 acetic acid, and a molar ratio of DES 60:1 YBaCu metal nitrates, at dehydrating temperatures of (a) 150 °C, (b) 180 °C, (c) 250 °C, and (d) 300 °C. (e) Table summarizing crystallite sizes values obtained per dehydrating temperature.

#### 2.7.2. Synthetic Performance of Choline Hydroxide 1:1 Pentanoic Acid, DES 30:1 YBaCu Metal Nitrates

Choline hydroxide 1:1 pentanoic acid, DES 30:1 YBaCu metal nitrates being held at different dehydration temperatures, provided the most contrasting and exciting results. Micromorphologically speaking, the reaction being dehydrated at 80 °C showed plate-like particles with an average crystallite size of 1151 nm. In contrast, despite the micromorphology likewise being plate-like particles (Figure 8a–d), the sizes of the crystallites analysed were significantly bigger, with average size values of 3178 nm at 150 °C, 4182 nm at 180 °C, and 2352 nm at 300 °C (Figure 8e). Additionally, maximum crystallite sizes can exemplify even further those differences, with values being 1576 nm at 80 °C, 7359 nm at 150 °C, 15,467 nm at 180 °C, and 4482 nm at 300 °C (Figure 8e). Similarly to what was observed with the DES made with acetic acid and being held at different dehydration temperatures, the synthetic performance presented by choline hydroxide 1:1 pentanoic acid, DES 30:1 YBaCu metal nitrates, also decreases compared to the obtained at 80 °C with 90% of the total phase percentage belonging to the metal oxide, with corresponding values of total phase percentage of 83% at 150 °C, 78% at 180 °C, 74% at 250 °C, and 80% at 300 °C (Figure 8e). Finally, analogue to the results previously described by the DES formed with acetic acid and dehydration temperature of 250 °C,

the micromorphology exhibited by choline hydroxide 1:1 pentanoic acid, DES 30:1 YBaCu metal nitrates, also displayed lower dimensions crystallites, around 101 nm in size (Figure 8e), and much bigger flat-like particles (Figure 8b), with sizes around 3827 nm (Figure 8e).

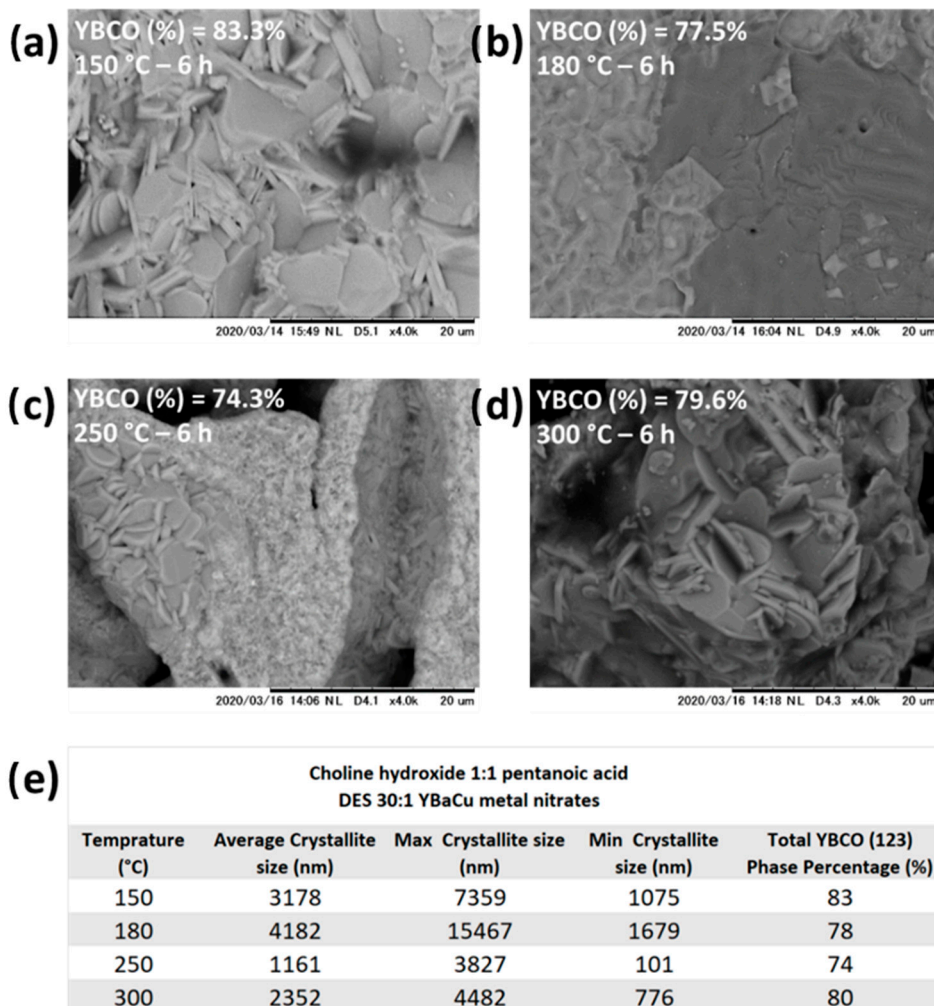


**Figure 8.** (a–d) SEM micrographs showing the morphology exhibited by the crystallites, synthesised using choline hydroxide 1:1 pentanoic acid, and a molar ratio of DES 30:1 YBaCu metal nitrates, at dehydrating temperatures of (a) 150 °C, (b) 180 °C, (c) 250 °C, and (d) 300 °C. (e) Table summarizing crystallite sizes values obtained per dehydrating temperature.

#### 2.7.3. Synthetic Performance of Choline Hydroxide 1:1 Nonanoic Acid, DES 20:1 YBaCu Metal Nitrates

Morphological behaviour exhibited by the use of choline hydroxide 1:1 nonanoic acid, DES 20:1 YBaCu metal nitrates, can be easily described by an almost constant crystal growth with an increase of the dehydration temperature, going from 1059 nm at 80 °C, to 1850, 1194, 2036, and 2774 nm obtained at 150, 180, 250, and 300 °C, respectively (Figure 9e). For temperatures ranging from 150 to 250 °C, the morphology of the crystallites can be described as plate-like particles, added to much smaller shapeless crystals (Figure 9a–c). The plate-like particles became heavily predominant at 300 °C (Figure 9d). In terms of the synthetic performance, unfortunately and similarly to results previously described by dehydration processes being carried out at different temperatures than 80 °C, is also hampered, providing values of 77%, 74%, 77%, and 70% of the total phase percentage belonging to the desired metal oxide, for dehydration temperatures of 150, 180, 250, and 300 °C, correspondingly (Figure 9e).

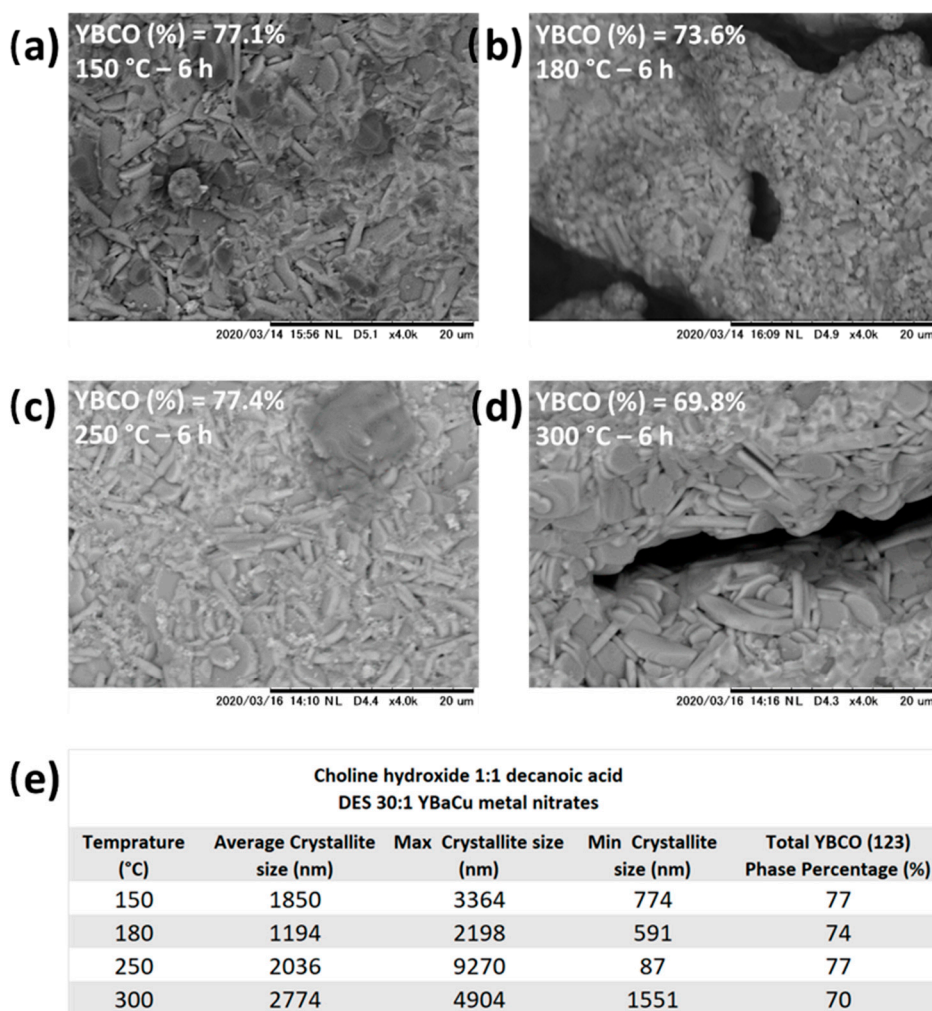


**Figure 9.** (a–d) SEM micrographs showing the morphology exhibited by the crystallites, synthesised using choline hydroxide 1:1 pentanoic acid, and a molar ratio of DES 30:1 YBaCu metal nitrates, at dehydrating temperatures of (a) 150 °C, (b) 180 °C, (c) 250 °C, and (d) 300 °C. (e) Table summarizing crystallite sizes values obtained per dehydrating temperature.

### 3. Scientific Discussion and Conclusions

The synthesis of the metal oxide YBCO (123), carried out by using choline hydroxide as the source of the cation, and molecules of different size containing the same anion, namely acetic acid, propionic acid, butyric acid, pentanoic acid, nonanoic acid, and decanoic acid, added to different molar ratios between the DES and the metal nitrates, delivered interesting results in terms of synthetic performance and the morphology displayed by the resulting crystallites. As for the former, a clear tendency towards better synthetic performance with the increase of the alkyl chain length of the molecule containing the anion, was observed, however, only to the point of butyric acid, which delivered the highest phase percentage obtained of the metal oxide, amongst all. From that point onwards, i.e., pentanoic acid to decanoic acid, a constant decay in total phase percentage belonging to the desired metal oxide is seen.

Also, morphological results were noted for every DES with molar ratios of DES ( $X$ ):1 YBaCu metal nitrates mixes, with  $x$  values of  $20 \leq x \leq 60$ . For DES formed by choline hydroxide 1:1 propionic/pentanoic/nonanoic/decanoic acid, the crystal formation is described by the production of bigger crystallites at lower  $x$  values, and sizes will decay in dimensions towards higher  $x$  values. The two exceptions were by using acetic acid, which crystallite size actually increases with increases in  $x$  values, and butyric acid, exhibiting low variation in crystallite sizes along the whole  $x$

spectrum. Our hypothesis of crystal formation, especially for DESs formed by choline hydroxide 1:1 propionic/pentanoic/nonanoic/decanoic acid is that, metal chelated nanoparticles shrouded by the inherent structure of the DES, will interact with ease while solvent/metal nitrates molar ratios are closer, i.e.,  $20 < x < 30$ , deriving in plate-like particles, whereas greater distance between metal nanoparticles will be generated by increasing  $x$  values, generating a highly spaced/diluted reaction environment, explaining the production of lower in dimensions crystallites. This is also more notorious when the DES is made by larger anions, such as nonanoic acid and decanoic acid. As for the DES formed with acetic acid, we believe that acetic acid, being relatively small compared to the others used in this work, is not affected and in fact, the chelated metal nanoparticles might be greater stabilised, perhaps also bigger in size, with  $x$  values closer to 60 than the opposite, therefore morphologically speaking, generating bigger crystallites with larger  $x$  values. This hypothesis is also supported by the fact that synthetic performance improved with  $x$  values increasing. Finally, the DES synthesised using butyric acid, which not only provided the best synthetic performance results, but also delivered relatively low variation in crystallite sizes, compared with all the results provided by the other DES. We believed that the interaction between choline hydroxide and butyric acid might be the most optimal, hence great synthetic performance results and low variation in crystallite sizes were displayed. However, more work needs to be done to prove this hypothesis.

The synthesis of the metal oxide with DES formed by choline hydroxide 1:1 acetic/pentanoic/nonanoic acid, and DES (X):1 YBaCu metal nitrates mixes, with  $x$  values of 60 for acetic acid, 30 for pentanoic acid, and 20 for nonanoic acid, and variations of the dehydration temperature, viz. 150, 180, 250, and 300 °C, also provided results of great value. In the vast majority of the results plate-like particles were observed. This is not estranged as it can be explained by a process denominated evaporation-based nanocrystal self-assembly [14]. Essentially, the assembly of colloidal nanocrystals can be forced by evaporation of the carrier solvent. Therefore, with boiling points of 117.9 °C for acetic acid, 186 °C for pentanoic acid, 254 °C for nonanoic acid, and 305 °C for choline hydroxide, and dehydration temperatures of 150, 180, 250, and 300 °C, thin plate-like particles were expected. However, there are a few exceptions that need to be noted. Firstly, for DES with acetic acid and pentanoic acid, and the dehydration process being done at 250 °C, above acetic acid and pentanoic acid boiling points, instead of elongated plate-like particles, in bot reactions crystallites of contrasting small size, compared to those seen at different temperatures, are observed. Our assumption is that, at this point the interaction between the anion and cation has been heavily destabilised, perhaps by the significant loss by evaporation of acetic acid and pentanoic acid, consequently producing such small-sized crystallites. Secondly, DESs being formed with pentanoic acid exhibited a phenomenal size growth of thin plate-like particles at 150 °C. The fact that the dehydration temperature was closed to pentanoic acid boiling point, allowed a controlled evaporation of one of the DES components, forcing the interaction of crystallites and prompting them to fuse. Unfortunately, we did not have access to techniques such as SEM-EDx (Energy Dispersive X-ray)-EBSD (Electron Back Scatter Diffraction) to further analyse the elemental distribution and plane growth of the sample however, results are promising to areas that require surface texturization and perhaps for the production of thin films. Finally, samples dehydrated at 300 °C, above acetic acid, pentanoic acid, and nonanoic acid boiling points, displayed plate-like particles of considerable size, hinting towards the fact that morphological results might be directed by the cation. The synthetic performance obtained in this last section was always lower than those results exhibited by carrying the dehydration process at 80 °C, which goes in agreement with the fact that early evaporation of the acid disrupts the overall chelating ability of the DES, therefore generating lower phase percentages of the desired metal oxide.

Briefly, the synthesis of  $\text{YBa}_2\text{Cu}_3\text{O}_{7-x}$  (YBCO or 123) was carried out successfully via various DESs here presented. The best synthetic performance among all was displayed by choline hydroxide 1:1 butyric acid, providing up to 93% of total phase percentage belonging to the superconductor. In terms of morphological results, plate-like particles are majorly seen along the whole synthetic series. Furthermore, for the cases of  $\text{C}_n\text{H}_{2n+1}$  with  $n = 3, 5, 9$ , and 10, bigger crystallites are produced with

$x$  values being lower, and sizes will decay in dimensions towards higher  $x$  values. For the synthesis of  $\text{YBa}_2\text{Cu}_3\text{O}_{7-x}$  (YBCO or 123) carried out at different initial dehydration temperatures, plate-like particles are the most predominant morphology observed, which agrees with the principle of evaporation-based nanocrystal self-assembly.

#### 4. Experimental Section

##### 4.1. Materials

Choline hydroxide (292257), acetic acid (695092), propionic acid (402907), butyric acid (B103500), pentanoic acid (240370), nonanoic acid (N29902), decanoic acid (C1875), barium nitrate (217581), and copper(II) nitrate trihydrate (V800130) are from Sigma-Aldrich (Tokyo, Japan), whereas yttrium(III) nitrate hexahydrate (150316) is from High Purity Chemicals Japan. Deionised water was obtained using a MilliQ PureLab Ultra ( $18.2 \text{ M} \Omega \text{ cm}^{-1}$ ). None of the materials required further purification and were used as received. All the reactants were generously provided by Professor Tadachika Nakayama's laboratory.

##### 4.2. Generation of Aqueous Precursors

Yttrium nitrate (0.05 M), barium nitrate (0.1 M), and copper nitrate (0.15 M) were mixed in a vial with deionised water under stirring until all salts were dissolved.

##### 4.3. Generation of Metal-Containing Deep Eutectic Solvents (DESs)

For the generation of the metal containing solutions firstly, choline hydroxide was mixed with the respective acid, namely acetic, propionic, butyric, pentanoic acid, nonanoic, and decanoic, in a 1:1 molar ratio, forming the DES. The mix was left for an hour to ensure proper DES formation before mixing it with any metal cation. Then, for the purposes of this work, the DES under study was combined with yttrium, barium, and copper nitrates varying the molar ratio between the DES and the moles of  $\text{YBaCu}$  metal nitrates, viz. from DES 10:1  $\text{YBaCu}$  metal nitrates to DES 80:1  $\text{YBaCu}$  metal nitrates.

##### 4.4. Dehydration of DES X:1 $\text{YBaCu}$ Metal Nitrates Mix

Dehydration of the mix was carried out at  $80^\circ\text{C}$  for 6 h without stirring the solution. However, specifically for the analysis performed at initial special conditions, dehydration was performed at different temperatures, i.e., 150, 180, 250, and  $300^\circ\text{C}$  for 6 h.

##### 4.5. Heating Protocols

All the dehydrated mixes of DES X:1  $\text{YBaCu}$  metal nitrates were calcined following the same calcination route: max temperature  $920^\circ\text{C}$ , at a ramp rate of  $5^\circ\text{C}/\text{min}$  with a dwell time at maximum temperature of 2 h.

##### 4.6. Characterization

Powder samples were analysed via powder X-ray diffractions (pXRD), obtained using a Rigaku RINT2000 diffractometer ( $\text{CuK}\alpha$  1 radiation at  $\lambda = 1.5418 \text{ \AA}$ ). To evaluate the composition of the resulting powders, Rietveld analysis was performed via Profex 3.12.1 Software [24]. The diffraction patterns were analysed using crystallographic information provided by the Inorganic Crystal Structure Database (ICSD). The reference numbers used for phase identification can be found in (Table S1). Morphological characterisation of the samples was carried out by Scanning Electron Microscopy (SEM) on a FE-SEM JEOL JSM 6700F. Finally, size distribution measurements were done via ImageJ software [25].

**Supplementary Materials:** The following are available online at <http://www.mdpi.com/1/1/4/s1>. The reference numbers used for phase identification can be found in (Table S1). Also, histograms of every SEM image can be

found in Figures S1–S9. Figure S10 shows results obtained with DES made of choline hydroxide 1:1 decanoic acid. Tables S2–S7 summarised total phase percentages, obtained via Rietveld refinement, belonging to YBCO (123) and other crystal compositions uncovered in the powder diffraction patterns.

**Author Contributions:** O.G.R. carried out experiments, data collection and writing of the article. T.N. provided valuable guidance and important discussion which made possible the writing of this article. T.N. also provided chemicals and equipment used for this work. All authors have read and agreed to the published version of the manuscript.

**Funding:** This research received no external funding.

**Acknowledgments:** O.G.R. would like to thank Thi Mai Dung for valuable discussions. O.G.R. would also like to thank WISE program for funding.

**Conflicts of Interest:** The authors declare no conflict of interest. The funders had no role in the design of the study; in the collection, analyses, or interpretation of data; in the writing of the manuscript, or in the decision to publish the results.

## References

- Ogale, S.B.; Venkatesan, T.V.; Blamire, M.G. *Functional Metal Oxides: New Science and Novel Applications*; Wiley-VCH: Weinheim, Germany, 2013; ISBN 978-3-527-33179-6.
- Xiang, X.-D.; Takeuchi, I. *Combinatorial Materials Synthesis*; Marcel Dekker: New York, NY, USA, 2003.
- Jorgensen, J.D.; Veal, B.W.; Paulikas, A.P.; Nowicki, L.J.; Crabtree, G.W.; Claus, H.; Kwok, W.K. Structural properties of oxygen-deficient  $\text{YBa}_2\text{Cu}_3\text{O}_{7-\delta}$ . *Phys. Rev. B* **1990**, *41*, 1863–1877. [[CrossRef](#)]
- Longo, E.; la Porta, F.D.A. *Recent Advances in Complex Functional Materials: From Design to Application*; Springer: New York, NY, USA, 2017; ISBN 3319538985.
- Lin, Y.H.; Nelson, J.; Goldman, A.M. Superconductivity of very thin films: The superconductor-insulator transition. *Phys. C Supercond. Appl.* **2015**, *514*, 130–141. [[CrossRef](#)]
- Wang, Y.; Zhang, M.; Lai, Y.; Chi, L. Advanced colloidal lithography: From patterning to applications. *Nano Today* **2018**, *22*, 36–61. [[CrossRef](#)]
- Fecht, H.J.; Hellstern, E.; Fu, Z.; Johnson, W.L. Nanocrystalline metals prepared by high-energy ball milling. *Metall. Trans. A* **1990**, *21*, 2333–2337. [[CrossRef](#)]
- Desbiolles, B.X.E.; Bertsch, A.; Renaud, P. Ion beam etching redeposition for 3D multimaterial nanostructure manufacturing. *Microsyst. Nanoeng.* **2019**, *5*, 1–8. [[CrossRef](#)] [[PubMed](#)]
- Singh, J.; Khan, S.A.; Shah, J.; Kotnala, R.K.; Mohapatra, S. Nanostructured  $\text{TiO}_2$  thin films prepared by RF magnetron sputtering for photocatalytic applications. *Appl. Surf. Sci.* **2017**, *422*, 953–961. [[CrossRef](#)]
- Danks, A.E.; Hall, S.R.; Schnepf, Z. The evolution of ‘sol-gel’ chemistry as a technique for materials synthesis. *Mater. Horiz.* **2016**, *3*, 91–112. [[CrossRef](#)]
- Qu, S.; Yu, Y.; Lin, K.; Liu, P.; Zheng, C.; Wang, L.; Xu, T.; Wang, Z.; Wu, H. Easy hydrothermal synthesis of multi-shelled  $\text{La}_2\text{O}_3$  hollow spheres for lithium-ion batteries. *J. Mater. Sci. Mater. Electron.* **2018**, *29*, 1232–1237. [[CrossRef](#)]
- Leng, J.; Wang, Z.; Wang, J.; Wu, H.H.; Yan, G.; Li, X.; Guo, H.; Liu, Y.; Zhang, Q.; Guo, Z. Advances in nanostructures fabricated: Via spray pyrolysis and their applications in energy storage and conversion. *Chem. Soc. Rev.* **2019**, *48*, 3015–3072. [[CrossRef](#)]
- Singh, J.; Dutta, T.; Kim, K.H.; Rawat, M.; Samddar, P.; Kumar, P. “Green” synthesis of metals and their oxide nanoparticles: Applications for environmental remediation. *J. Nanobiotechnol.* **2018**, *16*, 84. [[CrossRef](#)]
- Boles, M.A.; Engel, M.; Talapin, D.V. Self-assembly of colloidal nanocrystals: From intricate structures to functional materials. *Chem. Rev.* **2016**, *116*, 11220–11289. [[CrossRef](#)] [[PubMed](#)]
- Rojas, O.G.; Sudoh, I.; Nakayama, T.; Hall, S.R. The role of ionic liquids in the synthesis of the high-temperature superconductor  $\text{YBa}_2\text{Cu}_3\text{O}_{7-\delta}$ . *CrystEngComm* **2018**. [[CrossRef](#)]
- Celorrio, V.; Calvillo, L.; van den Bosch, C.A.M.; Granozzi, G.; Aguadero, A.; Russell, A.E.; Fermín, D.J. Mean Intrinsic Activity of Single Mn Sites at  $\text{LaMnO}_3$  Nanoparticles Towards the Oxygen Reduction Reaction. *ChemElectroChem* **2018**. [[CrossRef](#)]
- Rojas, O.G.; Nakayama, T.; Hall, S.R. Green and cost-effective synthesis of the superconductor BSCCO (Bi-2212), using a natural deep eutectic solvent. *Ceram. Int.* **2019**. [[CrossRef](#)]
- Rojas, O.G.; Song, G.; Hall, S.R. Fast and scalable synthesis of strontium niobates with controlled stoichiometry. *CrystEngComm* **2017**, *19*, 5351–5355. [[CrossRef](#)]

19. Maugeri, Z.; de María, P.D. Novel choline-chloride-based deep-eutectic-solvents with renewable hydrogen bond donors: Levulinic acid and sugar-based polyols. *RSC Adv.* **2012**, *2*, 421–425. [[CrossRef](#)]
20. Rojas, O.G.; Hall, S.R.; Nakayama, T. Synthesis of a Metal Oxide by Forming Solvate Eutectic Mixtures and Study of Their Synthetic Performance under Hyper- and Hypo-Eutectic Conditions. *Crystals* **2020**, *10*, 414. [[CrossRef](#)]
21. Green, D.C.; Glatzel, S.; Collins, A.M.; Patil, A.J.; Hall, S.R. A New General Synthetic Strategy for Phase-Pure Complex Functional Materials. *Adv. Mater.* **2012**, *24*, 5767–5772. [[CrossRef](#)]
22. Ma, Z.; Yu, J.; Dai, S. Preparation of Inorganic Materials Using Ionic Liquids. *Adv. Mater.* **2010**, *22*, 261–285. [[CrossRef](#)]
23. Perry, D.L. *Handbook of Inorganic Compounds*; CRC Press: London, UK, 1995; ISBN 9781439814611.
24. Doebelin, N.; Kleeberg, R. Profex: A graphical user interface for the Rietveld refinement program BGMLN. *J. Appl. Crystallogr.* **2015**, *48*, 1573–1580. [[CrossRef](#)]
25. Rueden, C.T.; Schindelin, J.; Hiner, M.C.; DeZonia, B.E.; Walter, A.E.; Arena, E.T.; Eliceiri, K.W. ImageJ2: ImageJ for the next generation of scientific image data. *BMC Bioinform.* **2017**, *18*, 529. [[CrossRef](#)] [[PubMed](#)]

**Sample Availability:** Samples of the compounds are available from the authors.

**Publisher’s Note:** MDPI stays neutral with regard to jurisdictional claims in published maps and institutional affiliations.



© 2020 by the authors. Licensee MDPI, Basel, Switzerland. This article is an open access article distributed under the terms and conditions of the Creative Commons Attribution (CC BY) license (<http://creativecommons.org/licenses/by/4.0/>).